Soil water nowcasting for site-specific yield potential estimation

Yi Yu, Mikaela J. Tilse, Patrick Filippi, and Thomas F. A. Bishop
Precision Agriculture, Hydrology & Geoinformation Science Laboratory, The University of Sydney, Australia

A paper from the Proceedings of the
17th International Conference on Precision Agriculture and 11th Brazilian Congress on Precision and Digital Agriculture
13-15 July 2026
Porto Alegre, Brazil

Abstract. *Knowing how much plant available water (PAW) is stored across a field at key decision points in the growing season is fundamental to precision agriculture. Spatial variability in soil water translates directly into variability in water-limited yield potential, yet most growers lack the tools to quantify this at the within-field scale. Here we present a Soil Water-Energy Balance (SWEB) model that offers a framework to deliver daily, 30 m resolution estimates of PAW across any dryland paddock in Australia, enabling spatially explicit pre and within-season yield potential mapping. SWEB combines two components: an energy balance and a water balance. The energy balance uses Landsat-derived Normalised Difference Vegetation Index (NDVI) and Land Surface Temperature to scale reference evapotranspiration (ET) from daily climate grids, producing spatially explicit daily ET estimates at 30 m resolution. The water balance applies Richards' equation to simulate vertical water movement through multiple soil layers, driven by precipitation, ET, and soil hydraulic properties derived from digital soil maps. The model is calibrated with downscaled Soil Moisture Active Passive (SMAP) soil moisture estimates (1 km spatial resolution). Two data scenarios are considered in terms of the underlying soil data: a data-limited scenario relying on national datasets such as the Soil-Landscape Grid of Australia (SLGA) and a data-abundant scenario incorporating on-farm soil maps derived from field sampling.*

Water-limited yield potential is estimated using the French and Schultz water-use efficiency framework, where yield potential equals water-use efficiency multiplied by available water minus losses. Available water integrates transpiration accumulated from the ET product up to a decision point, PAW from the water balance model at the decision point, and quantiles of climatological rainfall for the remainder of the season. This approach is illustrated for a 560 ha wheat paddock in eastern Australia, during the 2023 growing season, with nitrogen fertiliser decision points at sowing (22 May) and early stem elongation (Z31, 5 June).

Results showed that the on-farm soil map (data-abundant scenario) produced more spatially detailed PAW estimates compared to SLGA (data-limited), with whole-profile improvements in accuracy of 10 mm and bias of 9.6 mm. Both data scenarios generated yield potential maps with spatial patterns broadly consistent with observed 2023 yield map, with the data-abundant scenario capturing within-paddock variability more effectively. Across 178 independent soil moisture probe sites nationally, the SWEB model achieved a median correlation of 0.73 and

The authors are solely responsible for the content of this paper, which is not a refereed publication. Citation of this work should state that it is from the Proceedings of the 17th International Conference on Precision Agriculture and 11th Brazilian Congress on Precision and Digital Agriculture. EXAMPLE: Last Name, A. B. & Coauthor, C. D. (2026). Title of paper. In Proceedings of the 17th International Conference on Precision Agriculture and 11th Brazilian Congress on Precision and Digital Agriculture (unpaginated, online). Monticello, IL: International Society of Precision Agriculture and Brazilian Congress on Precision and Digital Agriculture.

median accuracy of 0.07 v/v. These results demonstrate that spatially variable, water-limited yield potential maps can be generated operationally for any dryland paddock in Australia at 30 m resolution with 5–10 days latency. This capability supports improved in-season decisions around nitrogen management, crop variety selection, and input allocation, and provides a foundation for integrating soil water nowcasting into precision agriculture platforms.

The data-limited approach can be applied globally as it is based on NASA remote sensing platforms (Landsat, SMAP) and there are both global and country-specific options for soil and weather grids equivalent to the Australia versions used here.

Keywords. *root-zone soil moisture; crop evapotranspiration; precision agriculture; yield potential*

Introduction

Water availability in the crop root zone is one of the primary determinants of crop growth, yield formation, and water-use efficiency across Australian grain-growing regions. While rainfall provides the primary input of water, crop performance is governed by the balance between root-zone soil moisture (RZSM), which represents water stored within the depth accessible to roots, and crop evapotranspiration (ET), which represents the combined water loss through plant transpiration and soil evaporation. Understanding both variables, and their interaction, is essential for effective monitoring of crop water status for better decision making.

In practice, substantial within-field variability in RZSM and ET is commonly observed due to spatial differences in soil texture, soil depth, topography, and historical management. These variations can lead to markedly different crop water stress responses within the same paddock, even under uniform rainfall conditions. However, many existing monitoring approaches fail to capture this heterogeneity at scales relevant to farm management. Point-based soil moisture measurements provide direct information on RZSM but are spatially sparse and difficult to upscale, while regional satellite or model-based products often operate at resolutions too coarse to resolve paddock-scale variability.

Remote sensing has improved the ability to monitor actual ET at high spatial resolution, providing valuable insight into crop water use and stress conditions (Anderson et al., 2012; Senay et al., 2013). ET integrates atmospheric demand, crop condition, and soil water availability, making it a powerful indicator of agricultural water stress. However, ET alone does not directly quantify how much water remains available to crops in the soil profile. Without an explicit representation of RZSM, it can be difficult to distinguish between short-term atmospheric effects and longer-term soil water limitations, particularly during critical growth stages. RZSM, by contrast, provides a direct measure of the water available for crop uptake and is strongly linked to yield variability and drought impacts (McNally et al., 2017; Seneviratne et al., 2010). Yet RZSM cannot be directly observed from satellites at the spatial and temporal resolutions required for agricultural decision-making. As a result, there is a clear need for modelling approaches that combine satellite-derived ET information with physically based representations of soil water dynamics, enabling consistent estimation of both ET and RZSM across scales.

To address this gap, the Sydney Soil Water-Energy Balance (SWEB) model was developed by explicitly linking surface energy processes with subsurface soil water balance processes. By using satellite-informed estimates of actual ET as a key driver of soil water depletion, SWEB ensures that crop water use reflects real crop and atmospheric conditions. At the same time, the soil water balance component tracks infiltration, storage, redistribution, and drainage within the root zone, allowing estimation of how long available soil water can sustain crop demand. For Australian agriculture, a scalable framework such as SWEB supports improved monitoring of within-field and regional water dynamics, enhanced understanding of spatial drivers of crop stress, and more informed management of water-limited systems.

In this work we illustrate the present SWEN and illustrate its use for making pre- and in-season estimates of seasonal yield potential using water-use efficiency equations (French and Schultz, 1984).

The Sydney soil water-energy balance (SWEB) model

SWEB is a process-based modelling framework developed to estimate daily within-field crop ET and RZSM by integrating satellite observations, weather data, and soil physical properties. The model is designed to support agricultural water management by providing spatially explicit information on soil water availability and crop water stress across farming systems. SWEB consists of two tightly coupled components: a surface energy balance (SEB) component that estimates actual ET, and a soil water balance (SWB) component that simulates water storage and movement within the soil profile.

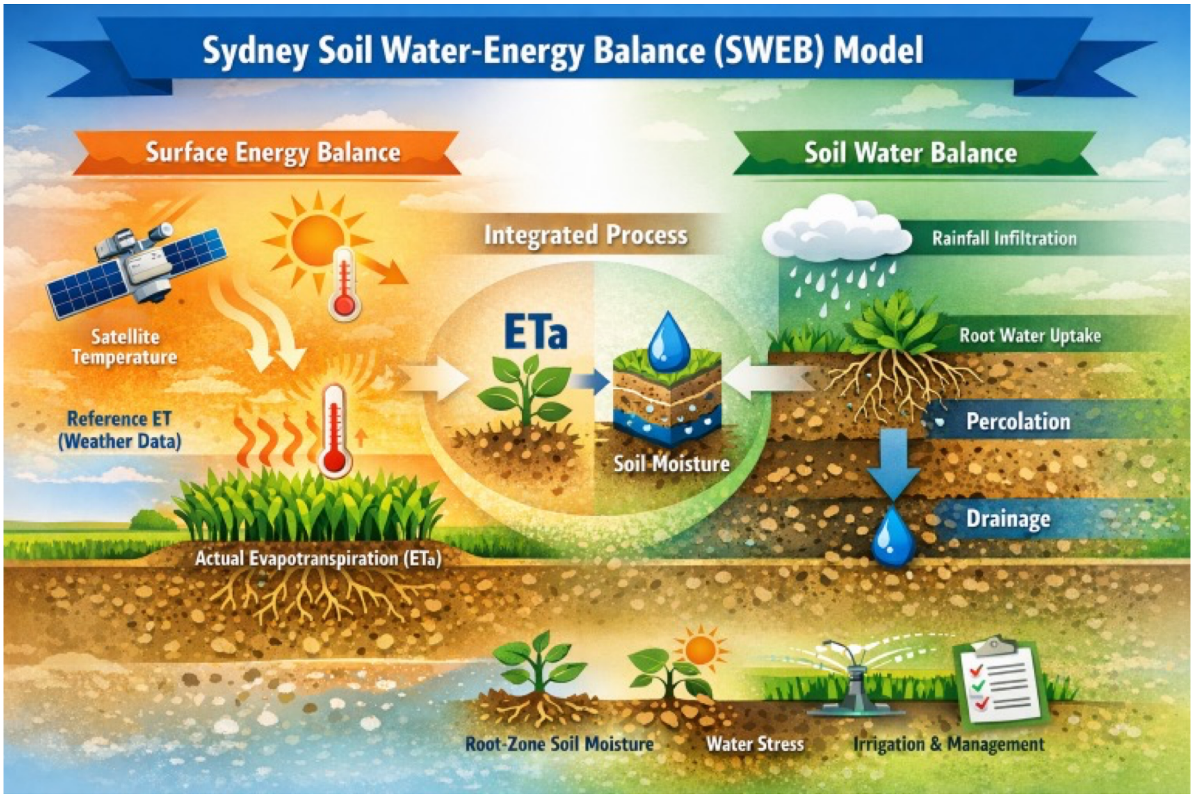

Fig. 1. Artwork illustrating the SWEB components (generated by ChaGPT).

SEB component: estimation of crop water use

The energy component of SWEB estimates actual ET, which represents the total water loss from the land surface through plant transpiration and soil evaporation. This component is driven by satellite-derived land surface temperature (LST) from the Landsat 8/9 missions (Irons et al., 2012; Roy et al., 2026), which provide thermal observations at a spatial resolution (100 m, resampled to 30 m) suitable for resolving within-field variability in Australian grain systems. Landsat LST is combined with gridded meteorological inputs from the SILO database (Jeffrey et al., 2001), which supplies spatially consistent climate variables, including radiation, air temperature, vapour pressure, and FAO-56 reference evapotranspiration (ETo). Together, these datasets enable physically consistent estimation of actual ET (ETa) that reflects both crop condition and atmospheric demand at paddock-relevant scales.

In principle, the model determines how much of the available atmospheric demand for water is actually met by the crop–soil system. When crops are well-watered, canopy temperatures tend to be lower and ET approaches the reference rate; under water stress, canopy temperatures increase and ET is reduced. The crop ET is estimated by scaling a reference ET, following the operational simplified surface energy balance (SSEBop) model (Senay et al., 2013 2022):

$$ET_a = K_c \times ET_o \quad (1)$$

$$K_c = K_{cb} + K_e \quad (2)$$

where ET_o is the reference FAO56 ET obtained from the SILO weather grids (Jeffrey et al., 2001); K_c is the crop factor as described in (Allen et al., 1998), which can be divided into two components—K_{cb} (basal crop coefficient representing primarily plant transpiration) and K_e (evaporation coefficient that represents the contribution of evaporation from soil to total ET). The resulting ETa can be estimated at a resolution consistent with that of the input Landsat data, i.e., 30 m spatial resolution. The ETa estimates represent actual water use, rather than potential demand, and therefore account for limitations imposed by SM availability, crop condition, and management (e.g., irrigation).

SWB component: root-zone water dynamics

The soil water balance component of SWEB tracks how water enters, moves through, and is stored within the soil profile. The soil is represented as a series of vertical layers extending from the surface to the maximum rooting depth.

In a simplified version, soil water storage on a daily time step is updated based on:

$$RZSM_{t+1} = RZSM_t + I_t - ET_{a,t} \cdot f_{evap} - D_t \quad (3)$$

$$I_t = P_t \cdot C_{infil} \quad (4)$$

$$f_{evap} = \frac{K_e}{K_c} \quad (5)$$

where $RZSM_t$ is RZSM at day t (mm) and $RZSM_{t+1}$ is the RZSM on the next day; I_t is the rainfall infiltration into the soil (mm/day), which can be obtained from rainfall data P_t together with a infiltration coefficient C_{infil}; the SEB component $ET_{a,t}$ (mm/day) needs to be scaled by a soil evaporation fraction f_{evap}, which is the ratio between K_e and K_c; D_t is drainage/percolation out of the root zone (mm/day).

The model uses established soil physical relationships to represent how water moves between soil layers, accounting for soil texture, porosity, and hydraulic conductivity. SWEB is designed to be flexible with respect to soil inputs and can ingest any digital soil map (DSM) that provides basic textural information (e.g., sand and clay fractions) and soil depth. Soil hydraulic parameters are derived using pedotransfer functions (PTFs) (Saxton and Rawls, 2006), enabling consistent estimation of soil water retention and hydraulic conductivity across spatial scales. Upper limits on soil water storage ensure that soils cannot hold more water than their physical capacity, while drainage removes excess water beyond the root zone.

In the model the Soil and Landscape Grid of Australia (SLGA; Malone and Searle, 2021a, 2021b) is used as the baseline national soil dataset, allowing for the model to be applied anywhere. Where available, it is possible to use on-farm soil data such as digital soil maps (DSMs) generated from machine learning methods or geostatistics. On-farm soil data provides more realistic representation of soil hydraulic properties at the on-farm scale.

Integration of energy and water proceses

A key strength of SWEB is the explicit linkage between SEB (surface process) and SWB (subsurface process) dynamics. ETa estimated from the SEB component is used as a direct sink of water in SWB. In this way, crop water use is constrained both by atmospheric conditions and by the amount of water actually available in the soil. This integration allows SWEB to capture important agricultural processes, such as monitoring crop water use during dry periods and waterlogging, and differences in water availability across soil types and landscapes.

Calibration of SWEB

SWEB needs to be spatially calibrated to ensure optimal within-field simulation performance. The calibration of SWEB employs a differential evolution optimisation algorithm to estimate three key parameters: f_{evap}, C_{infil} and k_{diff}. The objective function minimises the root mean square error (RMSE) between observed and simulated SSM at 50 mm depth over a specified calibration period (based on SMAP – see below). Parameter bounds are constrained as follows:

- $f_{evap} \in [0,\ 1]$ representing the fraction of total ETa allocated to surface evaporation;
- $C_{infil} \in [0,\ 1]$ being a coefficient for precipitation infiltration into surface layer;
- $k_{diff} \in [0, 10^6]$ being a diffusivity scaling length factor in the Brooks-Corey formulation.

The optimisation process uses differential evolution with a population size of 10, maximum 30 iterations, and convergence tolerance of 10^{-3}, requiring a minimum of 30 valid observation points for reliable parameter estimation. Currently SWEB is calibrated against surface SM retrievals from the Soil Moisture Active Passive (SMAP) mission (Entekhabi et al., 2010), which is adjustable and can be calibrated to on-farm soil water sources such as SM probes.

Operation settings through National Computational Infrastructure (NCI)

SWEB has been deployed through Australia's NCI's Gadi supercomputer infrastructure to enable continental-scale RZSM modelling for Australia's grain growing regions (**Fig. 1**). SWEB's Python-based *ProcessPoolExecutor* architecture facilitates parallel execution across the national-scale SM monitoring sites (Figure 2), with each site calibration requiring independent optimisation runs that can be distributed across NCI's computing nodes. The outputs of SWEB could be distributed (subject to computational cost) as an open collection through the NCI Thematic Real-time Environmental Distributed Data Services (THREDDS) Data Service, providing supports for national agricultural and hydrological decision-makings.

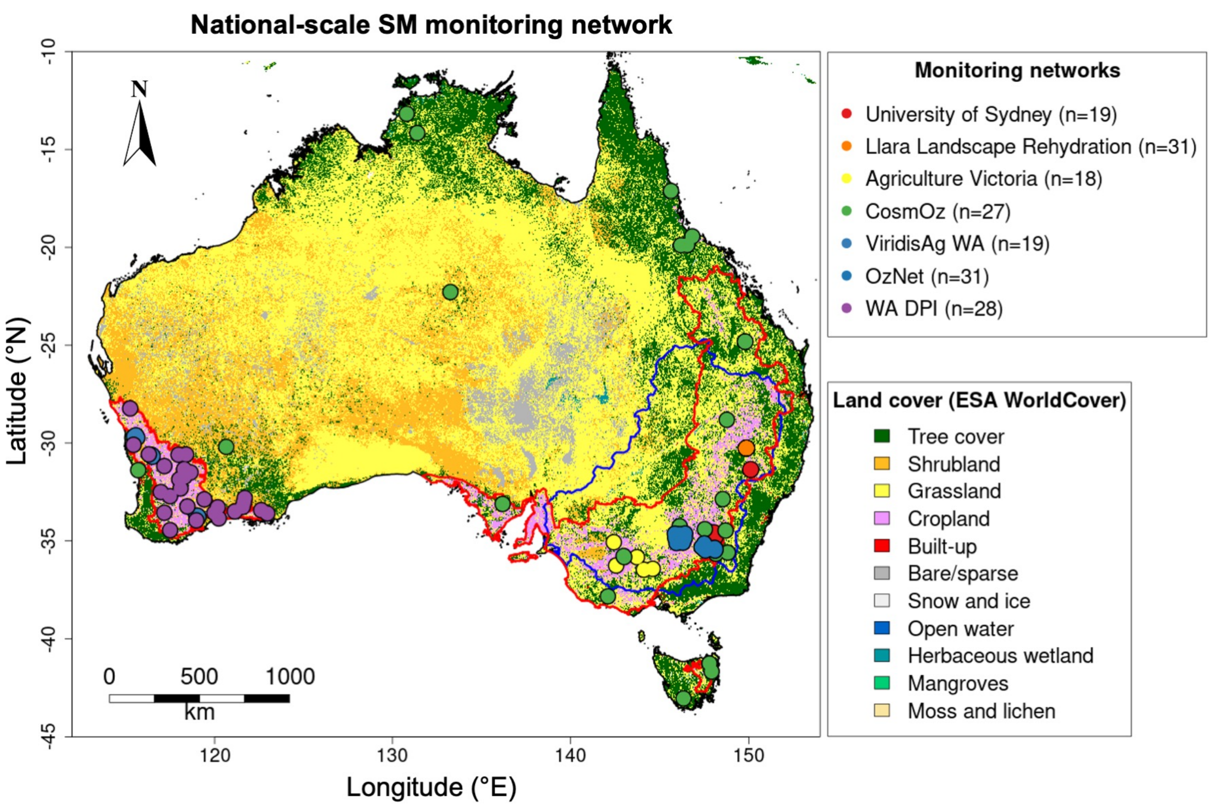

Fig. 1. The spatial distribution of a collated national-scale SM monitoring network for Australia. The dot points in various colours represent the sites from different SM monitoring networks. The land cover map is obtained from the ESA WorldCover 10 m v200 (Zanaga et al., 2022). The red

polygon delineates the grain growing regions.. The blue polygon delineates the Murray Darling Basin.

Validation of SWEB outputs

For the national-scale validation, the spatial distribution of SWEB's performance metrics across the Australia (Fig. 2) shows distinct national-scale patterns related to climate zones and landscape characteristics. RMSE values (panel a) display a clear longitudinal gradient with lowest errors (0.05-0.07) in western regions and higher errors (0.09-0.11) in southeast Australia. Correlation coefficients (panel b) show good performance (0.70-0.85) across most regions with highest correlations in southeast Australia, suggesting regional differences in model structure adequacy.

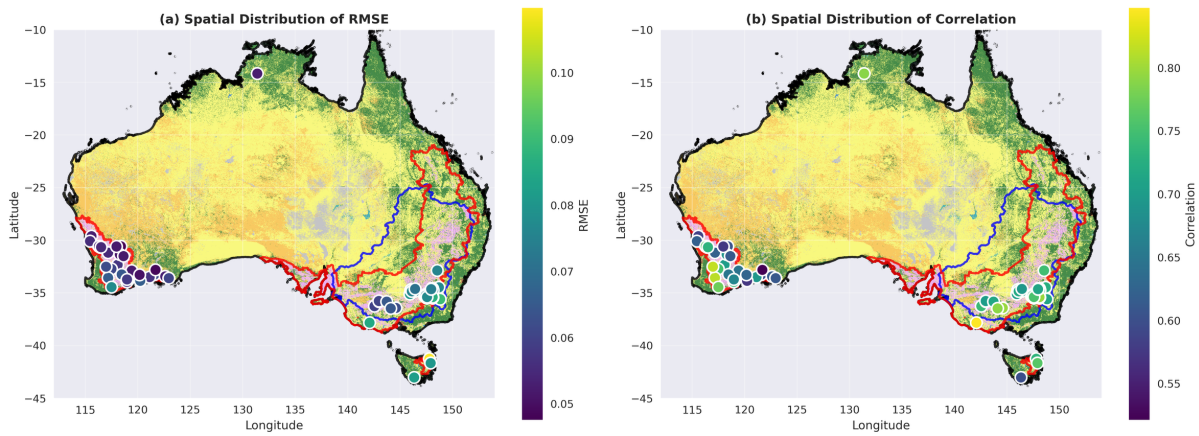

Fig. 2. National-scale spatial distribution of model performance metrics showing (a) RMSE and (b) correlation coefficient, with clear longitudinal gradients reflecting major climate zone transitions across Australia.

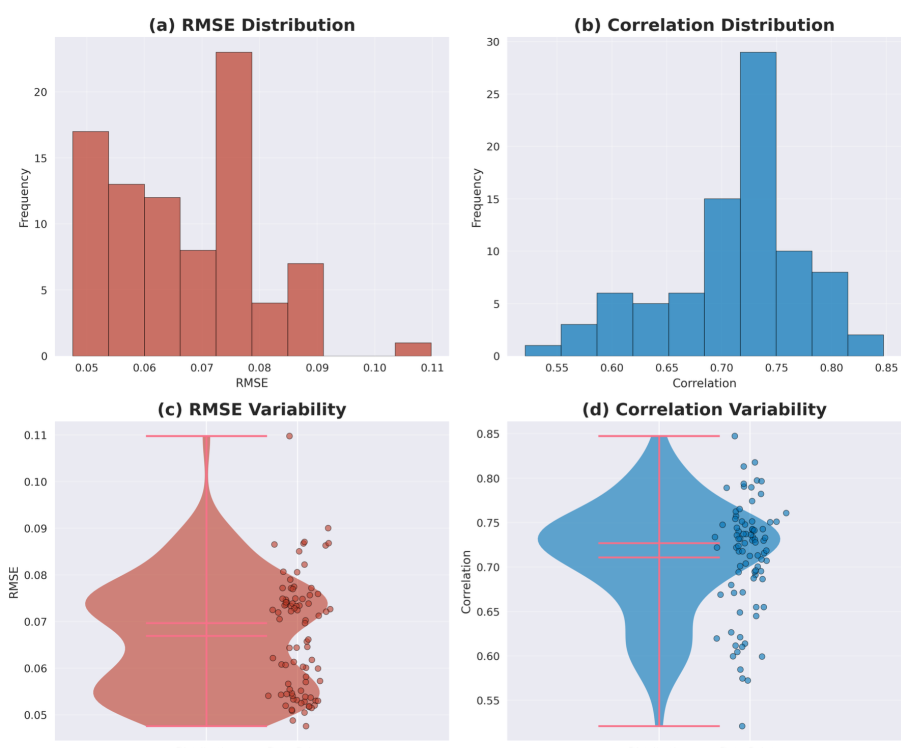

Fig. 3. (a–b) histograms and (c–d) violin plots showing national-scale frequency distributions and variability of model performance metrics (RMSE and correlation).

Model performance metric distributions at the national scale are displayed in Fig. 3. RMSE distribution (panel a, c) is dual-modal and centre-skewed with most values concentrated between 0.05-0.08, indicating consistently good model accuracy across diverse Australian conditions. Correlation distribution (panel b, d) shows a strong peak around 0.75 and minimal values below 0.55, demonstrating robust relationships across the continent.

Site-specific yield-potential estimation

A 560 ha wheat field in eastern Australia during the 2023 growing season was used to illustrate SWEB for site-specific yield-potential estimation. Figure 5 shows maps of whole-profile plant available water (0–1 m) for 22 April and 5 June 2023. These dates correspond to sowing and Z31, both of which are common times for nitrogen fertiliser application. Two estimates are presented: the first uses national digital soil maps (SLGA) to derive soil hydraulic properties, and the second uses on-farm digital soil maps (on-farm DSM). We refer to the first as the data-limited scenario and the second as the data-abundant scenario, in which a grower has invested in on-farm data collection. Assuming the on-farm DSM is correct, the root mean square error is 10 mm and the mean error is 9.6 mm for the SLGA. Furthermore, the PAW maps from the data-abundant scenario show more variability than those from the data-limited scenario.

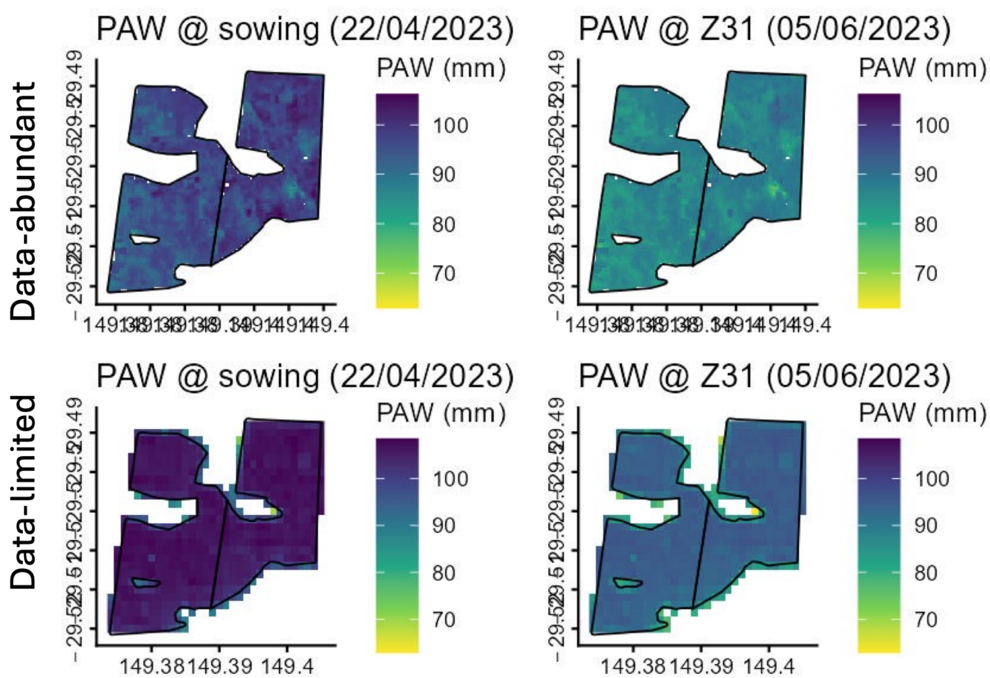

Fig. 5. Maps of whole-profile plant available water (0–1 m) at key decision points under the data-limited and data-abundant scenarios.

Water-limited yield potential in Australia is typically estimated for wheat using a water-use-efficiency equation where 23 kg grain yield per mm of water (French and Schultz et al., 1984). This is usually calculated from seasonal rainfall with a loss term of 110 mm to account for evaporation, runoff and excess drainage. Rather than using rainfall alone, we use the following to estimate available water:

- plant available water from SWEB at the decision point;
- the sum of transpiration (from SWEB) from sowing to the decision point; and

- climatology based on past records to estimate rainfall from the decision point to harvest. In the example below, we use a decile 2 rainfall (the 20th quantile rainfall based on historical records) as a conservative estimate of rainfall and water-limited yield potential.

The yield-potential maps are shown in Figure 6. Bias in the PAW estimates from the national soil data led to overestimation of yield potential compared with SWEB using on-farm soil data. Furthermore, when compared with the yield map, the national soil data produced relatively uniform yield-potential estimates, whereas the on-farm soil data captured more spatial variability. Therefore, for variable-rate nitrogen management, this example suggests that using SWEB with on-farm soil maps is preferable.

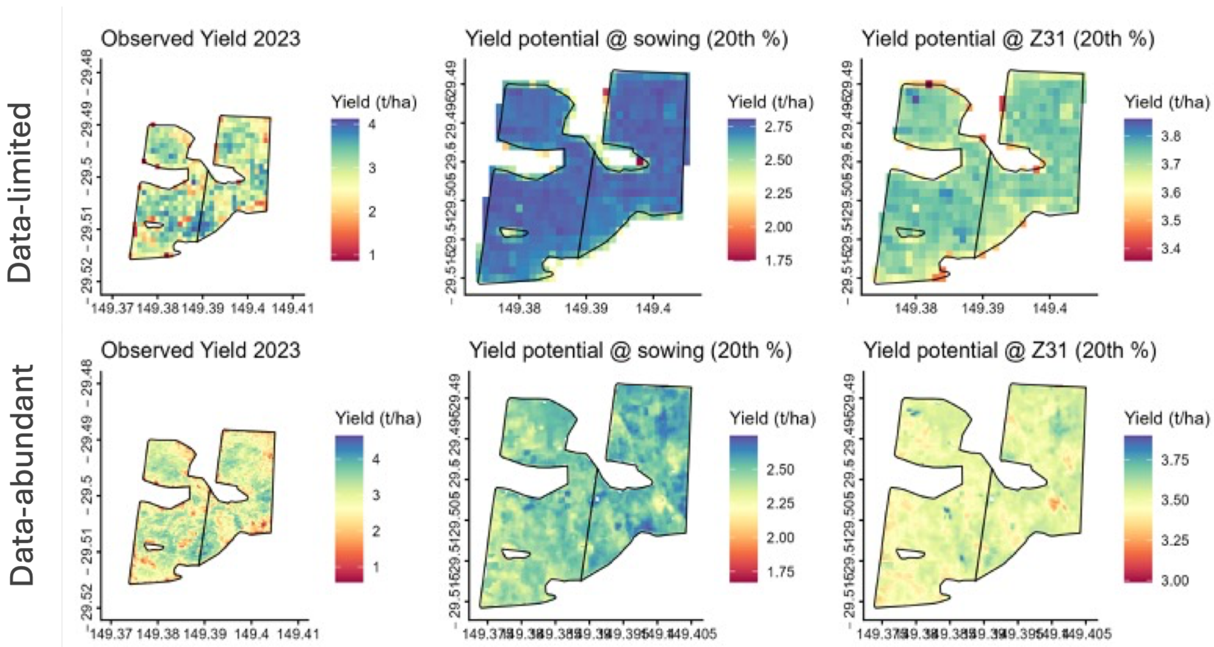

Fig. 6. Observed wheat yield and yield potential for each decision point in a data-limited and data-abundant scenario.

Conclusions

In this paper, we present SWEB, a practical and scalable modelling framework for monitoring crop water status across Australia's grain-growing regions by explicitly linking surface energy processes with subsurface soil water dynamics. By integrating high-resolution satellite observations, nationally consistent climate data, and physically based soil representations, SWEB provides spatially explicit estimates of ET and RZSM at paddock-relevant scales. A national-scale validation against multiple independent soil moisture monitoring networks shows that SWEB performs robustly across diverse climates, soils, and management systems, supporting confidence in its national applicability. Importantly, we illustrate how near-real-time estimates of PAW generated by SWEB create a direct pathway to yield forecasting, nutrient management, and risk-based decision making in water-limited environments.

Acknowledgments

The research undertaken as part of this project is made possible by the significant contributions of growers through both trial cooperation and the support of the Grains Research and Development Corporation (GRDC), and the authors thank them for their continued support. The authors also thank the custodians of the soil probe networks for making their data freely available for this research.

References

Allen, R.G., Pereira, L.S., Raes, D., Smith, M., 1998. Crop evapotranspiration - Guidelines for computing crop water requirements - FAO Irrigation and drainage paper 56. Food and Agriculture Organization of the United Nations, Rome.

Anderson, M.C., Allen, R.G., Morse, A., Kustas, W.P., 2012. Use of Landsat thermal imagery in monitoring evapotranspiration and managing water resources. Remote Sens. Environ. 122, 50–65. doi:10.1016/j.rse.2011.08.025.

Entekhabi, D., Njoku, E.G., Neill, P.E.O., Kellogg, K.H., Crow, W.T., Edelstein, W.N., Entin, J.K., Goodman, S.D., Jackson, T.J., Johnson, J., Kimball, J., Piepmeier, J.R., Koster, R.D., Martin, N., McDonald, K.C., Moghaddam, M., Moran, S., Reichle, R., Shi, J.C., Spencer, M.W., Thurman, S.W., Tsang, L., Zyl, J.V., 2010. The Soil Moisture Active Passive (SMAP) Mission. Proc. IEEE 98, 704–716. doi:10.1109/JPROC.2010.2043918

French, R., Schultz, J., 1984. Water use efficiency of wheat in a Mediterranean-type environment. I. The relation between yield, water use and climate. Aust. J. Agric. Res. 35, 743–764. doi:10.1071/AR9840743

Irons, J.R., Dwyer, J.L., Barsi, J.A., 2012. The next Landsat satellite: The Landsat Data Continuity Mission. Remote Sens. Environ. 122, 11–21. doi:10.1016/j.rse.2011.08.026

Jeffrey, S.J., Carter, J.O., Moodie, K.B., Beswick, A.R., 2001. Using spatial interpolation to construct a comprehensive archive of Australian climate data. Environ. Model. Softw. 16, 309–330. doi:10.1016/S1364-8152(01)00008-1

Malone, B., Searle, R., 2021a. Updating the Australian digital soil texture mapping (Part 1): re-calibration of field soil texture class centroids and description of a field soil texture conversion algorithm. Soil Res. 59, 419–434. doi:10.1071/SR20283

Malone, B., Searle, R., 2021b. Updating the Australian digital soil texture mapping (Part 2): spatial modelling of merged field and lab measurements. Soil Res. 59, 435–451. doi:10.1071/SR20284

McNally, A., Arsenault, K., Kumar, S., Shukla, S., Peterson, P., Wang, S., Funk, C., Peters-Lidard, C.D., Verdin, J.P., 2017. A land data assimilation system for sub-Saharan Africa food and water security applications. Sci. Data 4, 170012. doi:10.1038/sdata.2017.12

Roy, D.P., Wulder, M.A., Gorelick, N., Hansen, M., Healey, S., Hostert, P., Huntington, J., Radeloff, V.C., Scambos, T., Schaaf, C., Woodcock, C.E., Zhu, Z., 2026. The next Landsat: Mission turning point? Remote Sens. Environ. 332, 115087. doi:10.1016/j.rse.2025.115087

Saxton, K.E., Rawls, W.J., 2006. Soil Water Characteristic Estimates by Texture and Organic Matter for Hydrologic Solutions. Soil Sci. Soc. Am. J. 70, 1569–1578. doi:10.2136/sssaj2005.0117

Senay, G.B., Bohms, S., Singh, R.K., Gowda, P.H., Velpuri, N.M., Alemu, H., Verdin, J.P., 2013. Operational Evapotranspiration Mapping Using Remote Sensing and Weather Datasets: A New Parameterization for the SSEB Approach. JAWRA J. Am. Water Resour. Assoc. 49, 577–591. doi:10.1111/jawr.12057

Senay, G.B., Friedrichs, M., Morton, C., Parrish, G.E.L., Schauer, M., Khand, K., Kagone, S., Boiko, O., Huntington, J., 2022. Mapping actual evapotranspiration using Landsat for the conterminous United States: Google Earth Engine implementation and assessment of the SSEBop model. Remote Sens. Environ. 275, 113011. doi:10.1016/j.rse.2022.113011

Seneviratne, S.I., Corti, T., Davin, E.L., Hirschi, M., Jaeger, E.B., Lehner, I., Orlowsky, B., Teuling, A.J., 2010. Investigating soil moisture–climate interactions in a changing climate: A review. Earth-Sci. Rev. 99, 125–161. doi:10.1016/j.earscirev.2010.02.004

Zanaga, D., Van De Kerchove, R., Daems, D., De Keersmaecker, W., Brockmann, C., Kirches, G., Wevers, J., Cartus, O., Santoro, M., Fritz, S., Lesiv, M., Herold, M., Tsendbazar, N.-E., Xu, P., Ramoino, F., Arino, O., 2022. ESA WorldCover 10 m 2021 v200. doi:10.5281/ZENODO.7254221